Vadim Tsvankin, MD[*]
Rintaro Hashizume, MD, PhD[‡]
Hiroaki Katagi, MD[‡]
James E. Herndon, II, PhD[§]
Christopher Lascola, MD, PhD[¶]
Talaignair N. Venkatraman, PhD[¶]
Daniel Picard, MS[‖ #]
Brainard Burrus, BS[**]
Oren J. Becher, MD[‡‡ §§]
Eric M. Thompson, MD[* ¶¶]

[*]Department of Neurosurgery, Duke University Medical Center, Durham, North Carolina; [‡]Department of Neurosurgery, Northwestern University Feinberg School of Medicine, Chicago, Illinois; [§]Department of Biostatistics and Bioinformatics, Duke University, Durham, North Carolina; [¶]Department of Radiology, Duke University Medical Center, Durham, North Carolina; [‖]Department of Pediatric Oncology, Hematology, and Clinical Immunology, Medical Faculty, University Hospital Düsseldorf, Düsseldorf, Germany; [#]Department of Pediatric Neuro-Oncogenomics, German Cancer Consortium and German Cancer Research Center, Heidelberg, Germany; [**]University of North Carolina School of Medicine, Chapel Hill, North Carolina; [‡‡]Department of Pediatrics, Northwestern University Feinberg School of Medicine, Chicago, Illinois; [§§]Robert H. Lurie Comprehensive Cancer Center, Northwestern University, Chicago, Illinois; [¶¶]Duke University Preston Robert Tisch Brain Tumor Center, Durham, North Carolina

Portions of this work were presented as an oral abstract on May 1, 2018, at the 2018 American Association of Neurological Surgeons Annual Meeting in New Orleans, Louisiana.

Correspondence:
Eric M. Thompson, MD,
Duke University Medical Center,
2301 Erwin Rd., PO Box 3272,
Durham, NC 27710.
Email: eric.thompson@duke.edu

Received, October 8, 2018.
Accepted, February 23, 2019.
Published Online, June 21, 2019.

ABC Transporter Inhibition Plus Dexamethasone Enhances the Efficacy of Convection Enhanced Delivery in H3.3K27M Mutant Diffuse Intrinsic Pontine Glioma

BACKGROUND: An impermeable blood–brain barrier and drug efflux via ATP-binding cassette (ABC) transporters such as p-glycoprotein may contribute to underwhelming efficacy of peripherally delivered agents to treat diffuse intrinsic pontine glioma (DIPG).
OBJECTIVE: To explore the pharmacological augmentation of convection-enhanced delivery (CED) infusate for DIPG.
METHODS: The efficacy of CED dasatinib, a tyrosine kinase inhibitor, in a transgenic H3.3K27M mutant murine model was assessed. mRNA expression of ABCB1 (p-glycoprotein) was analyzed in 14 tumor types in 274 children. In Vitro viability studies of dasatinib, the p-glycoprotein inhibitor, tariquidar, and dexamethasone were performed in 2 H3.3K27M mutant cell lines. Magnetic resonance imaging (MRI) was used to evaluate CED infusate (gadolinium/dasatinib) distribution in animals pretreated with tariquidar and dexamethasone. Histological assessment of apoptosis was performed.
RESULTS: Continuous delivery CED dasatinib improved median overall survival (OS) of animals harboring DIPG in comparison to vehicle (39.5 and 28.5 d, respectively; $P = .0139$). Mean ABCB1 expression was highest in K27M gliomas. In Vitro, the addition of tariquidar and dexamethasone further enhanced the efficacy of dasatinib ($P < .001$). In Vivo, MRI demonstrated no difference in infusion dispersion between animals pretreated with dexamethasone plus tariquidar prior to CED dasatinib compared to the CED dasatinib. However, tumor apoptosis was the highest in the pretreatment group ($P < .001$). Correspondingly, median OS was longer in the pretreatment group (49 d) than the dasatinib alone group (39 d) and no treatment controls (31.5 d, $P = .0305$).
CONCLUSION: ABC transporter inhibition plus dexamethasone enhances the efficacy of CED dasatinib, resulting in enhanced tumor cellular apoptosis and improved survival in H3.3K27M mutant DIPG.

KEY WORDS: Diffuse intrinsic pontine glioma, Convection-enhanced delivery, Dasatinib, p-Glycoprotein, Dexamethasone, MRI, Apoptosis

Neurosurgery 86:742–751, 2020 DOI:10.1093/neuros/nyz212 www.neurosurgery-online.com

Diffuse intrinsic pontine glioma (DIPG) is an inoperable malignancy that accounts for nearly 10% of all childhood central nervous system tumors, and is the leading cause of brain–tumor-related death in children.[1] Despite intensive clinical and translational efforts, the median overall survival (OS) remains only 9 mo,[2] and clinical trials of

ABBREVIATIONS: ABC, ATP-binding cassette; **ANOVA,** analysis of variance; **BBB,** blood–brain barrier; **CED,** convection-enhanced delivery; **DIPG,** diffuse intrinsic pontine glioma; **DMSO,** dimethylsulfoxide; **FOV,** field of view; **GSEA,** Gene Set Enrichment Analysis; **HGG,** high-grade glioma; **IACUC,** Institutional Animal Care and Use Committee; **IP,** intraperitoneal; **MRI,** magnetic resonance imaging; **OS,** overall survival; **PDGFR,** platelet-derived growth factor receptor; **SD,** standard deviation; **TE,** echo time; **TR,** repetition time

Supplemental digital content is available for this article at www.neurosurgery-online.com.

systemic therapies have largely failed to improve outcomes.[1-3]

One explanation for the failure of peripherally delivered chemotherapeutic agents to provide survival benefit in children with DIPG is the heterogeneous pontine blood–brain barrier (BBB).[4,5] A tenacious BBB likely contributes to the lack of promising in Vitro studies translating into in Vivo and clinical efficacy. The BBB of DIPG and DIPG cells, themselves, also contains ATP-binding cassette (ABC) transporters, such as ABCC1 (MRP1),[2] that act as chemotherapeutic drug efflux pumps and may further limit therapeutic efficacy. Our group previously found that ABC knockout mice harboring DIPGs had elevated concentrations of the intraperitoneally delivered receptor tyrosine kinase inhibitor, dasatinib, in both normal brain and tumor compared to wild-type mice.[6] Furthermore, ABC transporter inhibition with tariquidar, a third generation p-glycoprotein inhibitor,[7] in combination with small molecules has been well tolerated in children with refractory systemic solid tumors and resulted in increased intratumoral drug accumulation.[8] Tariquidar has been shown to inhibit p-glycoprotein in multiple tumor types, resulting in increased small molecule concentrations and enhanced tumor cell death.[9-12]

Convection-enhanced delivery (CED) of therapeutics is a method to bypass the BBB. The feasibility of CED for DIPG has been shown in small numbers of children.[13-16] However, CED for the treatment of malignant gliomas has previously had limited success, and therapeutic infusate has typically not targeted specific genetic tumor drivers. Platelet-derived growth factor (PDGFR), a receptor tyrosine kinase, is the most commonly overexpressed oncogene in DIPG[17-23] and is therefore a rational therapeutic target. Dasatinib has significant effects against PDGFR, has shown in efficacy against DIPG in Vitro,[22-24] and demonstrated feasibility in an early clinical study of DIPG.[25] Furthermore, we have previously shown that dasatinib is a substrate of the multidrug resistance ABC transporter, p-glycoprotein.[6] The purpose of this study was to elucidate a putative relationship between ABC transporter inhibition and CED of small molecules in DIPG. We hypothesized that inhibition of p-glycoprotein in DIPG will enhance the efficacy of CED infusate containing dasatinib.

METHODS

Patient ABC Transporter Gene Expression

The R2 Genomics Analysis and Visualization Platform (http://r2.amc.nl) was used to investigate ABCB1 (p-glycoprotein) mRNA expression across pediatric brain and pediatric systemic solid tumors using a publicly available dataset.[26] Pathological diagnosis in that dataset was determined using whole genome sequencing.[26] Gene expression profiling of ABC transporters of 2 publicly available DIPG datasets[27,28] was performed using the "KEGG_ABC_TRANSPORTERS" gene set in Gene Set Enrichment Analysis (GSEA) software (Broad Institute) to determine if differences in gene ABC transporter expression exist between H3.3K27M mutant and wild-type tumors.

Cell Viability Assays

Two DIPG H3.3K27M mutant cell lines were used, SF7761 and HSJD-DIPG-007. For determination of cell viability effects of dasatinib and tariquidar, tumor cells were seeded in 96-well plates, at 2500 cells per well, and cultured in the presence of dasatinib and/or tariquidar and dexamethasone, with triplicate samples for each incubation condition. Relative numbers of viable cells were determined by MTS assay (Promega, Madison, Wisconsin). Inhibitor viability effects at 18, 24, 48, and 72 h were determined by MTS assay in the presence of IC50 concentrations of dasatinib (SF7761: 0.1 μM concentration, HSJD-DIPG-007: 2 μM concentration), IC50 concentrations of tariquidar (SF7761: 1 μM concentration, HSJD-DIPG-007: 1 μM concentration), and/or dexamethasone (10 μM concentration), as compared to treatment with vehicle (dimethylsulfoxide (DMSO)). Dexamethasone was explored given its widespread use in DIPG at diagnosis, during radiotherapy, and at recurrence.[29] The plots represent absorbance quantification (optical density, $\lambda = 490$ nm) (each point is an average of cell-culture replicates, $n = 3$). Error bars indicate standard deviation (SD).

Mice and RCAS/TVA Model of H3.3K27M DIPG

All animal studies were approved by the Institutional Animal Care and Use Committee (IACUC). The replication-competent avian leukosis virus long terminal repeat with splice acceptor tumor virus A (RCAS/TV-A) system was used to generate a DIPG model expressing an H3.3K27M mutation as previously described.[30] Briefly, Nestin TV-A mice were each crossed with $p53^{fl/fl}$ mice to create NTV-A; $p53^{fl/fl}$ mice. Mice additionally carried a stop-floxed luciferase gene, allowing for photonic emission detection as a surrogate for the emergence of clinically significant tumor burden. DF1 virus-producing cells (chicken fibroblasts) were transfected with RCAS plasmids (RCAS-PDGF-B, RCAS-Cre, and RCAS-H3.3K27M). Approximately 1 μL (1×10^5) of DF1 cells expressing RCAS-PDGF-B, RCAS-Cre, and RCAS-H3.3K27M at a 1:1:1 ratio were stereotactically injected into the brainstem of NTV-A; $p53^{fl/fl}$ mice as previously described.[31] Viruses selectively infect nestin-producing cells,[32] and the resulting tumor is histologically consistent with high-grade brainstem glioma, with gene expression similar to human samples.[33] Mice were monitored closely for signs of tumor development (lethargy, head tilt, and increased head size). Any animal showing signs of distress or morbidity, including > 25% weight loss, severe neurological deficit such as hemiparesis, or lethargy, was sacrificed.

Rodent Bioluminescent Imaging

Photonic emission detection using an IVIS Imaging System 100 Series (Xenogen, Alameda, California) was completed twice weekly after initial injection. 10 mg/mL of luciferin (3 mg/mL, Gold Biotechnology, St Louis, Missouri) in sterile PBS was administered by intraperitoneal (IP) injection, and imaging was completed 5 min later 25 cm from the photon detector. Bioluminescence from a predefined region of interest surrounding the head of each mouse was recorded in photons per min. Images were analyzed using Living Image software, version 4.50 (Xenogen, Alameda, California). Only animals with confirmed tumors ($\geq 1 \times 10^5$ p/s/cm^2/sr radiance on 2 consecutive scans) were included.

Magnetic Resonance Imaging

Magnetic resonance imaging (MRI) experiments were performed on a 7.0-T small-animal MRI scanner (Bruker BioSpin MRI GmbH, Ettlingen, Germany) with a 72-mm quadrature volume coil. The scanner was operated using Paravision 5.1 software (Bruker). During scanning,

animals were anesthetized using 1.5% isoflurane with 40% oxygen and 60% nitrogen, delivered via custom nose cone. The animals' core body temperatures were maintained at 37°C ± 0.5°C by a circulating water bath, and respiratory rates were maintained at 50 to 70 respirations per second. A T2-weighted fast spin-echo rapid acquisition with refocused echoes sequence was completed using the following parameters: field of view (FOV) = 2 × 2; matrix = 128 × 128; echo time (TE)/repetition time (TR) = 12/4200 ms; slices = 16; slice thickness = 0.5; scan time = 6 min 43 s. For CED infusate measurements, T1-weighted FLASH sequences were performed with the following parameters: FOV = 2 × 2; matrix = 128 × 128; TE/TR = 3/133 ms; excitation pulse angle = 60 degree; slice thickness = 0.5 mm; averages = 8; scan time = 2 min 16 s. The T1-weighted imaging parameters were as follows: TR/TE = 160 ms/1.6 ms, field of view = 3.2 × 3.2 cm^2, slice thickness = 1 mm, matrix = 256 × 256. Coronal images T1-weighted images were acquired 10 min following CED infusion and approximately every 10 min for 1 h. Time to peak T1-weighted signal intensity of gadoteridol was determined in the region of interest adjacent to the CED catheter tip using the DCE tool plugin (Kyung Sung, Los Angeles, California) for Horos (v2.0.0).

Convection-Enhanced Delivery

Animals were anesthetized by isoflurane inhalation and placed in a stereotactic frame (Model 900; David Kopf Instruments, Tujunga, California). A midline scalp incision was made to expose the lambdoid and sagittal sutures. A burr hole adequate for CED catheter entry was made 2 mm lateral to the lambda. For animals treated by continuous CED pump, the incision was extended posteriorly to accommodate subcutaneous insertion of the delivery pump (Model No. 2002, ALZET, Cupertino, California) capable of delivering 100 μL of infusate at 0.5 μL/h over 14 d, for a total 2 μM infusion. Pumps were filled with infusate, coupled to a right angle catheter, and primed as per manufacturer's instructions 24 h prior to implantation. Catheters were mounted to a custom stereotactic insertion arm by the connecting bracket, and lowered using the stereotactic frame to a final depth of 4.5 mm beyond the outer table of the skull. The mounting bracket was secured to the skull with veterinary glue, disconnected from the stereotactic arm, and the skin was closed using 4-0 nylon suture. For the continuous CED infusion, animals received either CED 2 μM dasatinib at 0.5 μL/h over 14 d or CED vehicle (0.9 NaCl with 1% DMSO at 0.5 μL/h). Of note, because dasatinib is not FDA approved for delivery via CED, it is considered off label.

A separate single-dose CED infusion study was completed to allow for the MRI analysis of infusate. For animals treated with single-dose infusion, a 33-gauge needle gas-lock Hamilton syringe was secured to an UltraMicroPump III (World Precision Instruments, Sarasota, Florida) and mounted onto the stereotactic frame. A total of 2 μM dasatinib and 100 μM gadoteridol solution were preloaded into the Hamilton syringe. The needle was lowered to a final depth of 4.5 mm beyond the outer table of the skull. The infusate was delivered at 0.5 μL/min for 10 min for a total infusate volume of 5 μL. The needle was slowly retracted 5 min after completion of the infusion, and the skin was closed with 4-0 nylon suture. The animal was removed from the frame and immediately taken to MRI under anesthesia. The molecular weight of dasatinib is 488 D; comparably, gadoteridol is 558 D, which reasonably correlates with comparably sized molecules for MRI assessment of distribution volume.[34] For the single-dose CED study, animals received one of the following: (1) CED dasatinib (2 + 100 μM gadoteridol at 0.5 μL/min, total infusate volume 5 μL); (2) IP dexamethasone (0.5 mg/kg) plus IP tariquidar (Selleckchem, Houston, Texas) (5 mg/kg), followed 45 min later by CED dasatinib (2 + 100 μM gadoteridol at 0.5 μL/min, total infusate volume 5 μL); or (3) no treatment. A study of CED infusion of dasatinib, dexamethasone, and tariquidar was not performed given the small volume of the mouse pons.

Immunohistochemistry

All experimental animals were sacrificed in accordance with IACUC standards of care. After harvest, brains were further fixed in 10% formalin at room temperature for 1 wk before being processed and embedded in paraffin. Sections were cut at a thickness of 5 μm, and stained with standard hematoxylin and eosin staining to confirm tumor. Specimens are deparaffinized and underwent antigen retrieval at pH 6.1 at 100°C for 20 min. Specimens were stained for cleaved caspase 3, a marker of cellular apoptosis[35] (CC3; Cell Signaling Technology 9664S, Danver, Massachusetts) at 1:800 dilution, and Ki67, a marker of cellular proliferation (Thermo Fisher Scientific RM9106, Waltham, Massachusetts) at 1:300 dilution. Secondary antibody was VECTASTAIN ABC (Vector Laboratories PK-7100, Burlingame, California). Images were acquired at 10x using an Olympus (Tokyo, Japan) CKX41 microscope and DP25 camera (Carl Zeiss, Jena, Germany). Positive-staining cells were quantified using FIJI (NIH, Bethesda, Maryland).

Statistical Analysis

Kaplan–Meier curves graphically described the survival of mice treated with and without various treatments. The generalized Wilcoxon test compared treatment groups with respect to OS using SAS (Cary, North Carolina). mRNA expression was compared using analysis of variance (ANOVA) with Tukey's multiple comparisons using SAS. Using GraphPad Prism v5.0 software (La Jolla, California), ANOVA with Tukey's multiple comparisons was used to explore the impact of adding tariquidar and dexamethasone to dasatinib on in Vitro viability. ANOVA compared treatment groups with respect to the number of CC3 and Ki67 positive cells per high-power field. P values $\leq .05$ were considered significant.

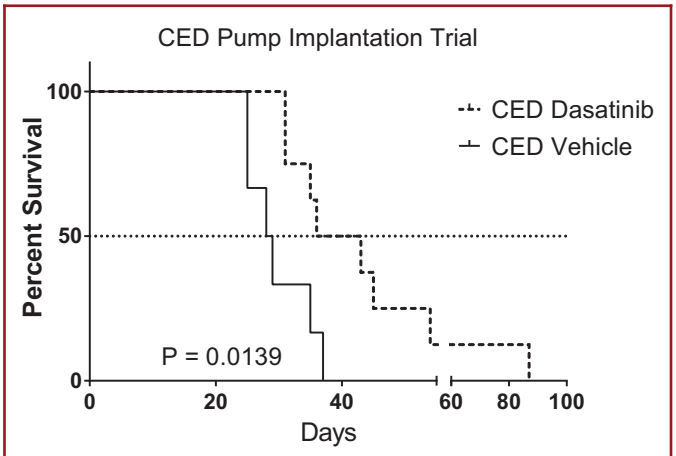

FIGURE 1. *Kaplan–Meier curve of tumor-bearing mice treated with continuous CED infusion of dasatinib or continuous CED infusion of vehicle. CED dasatinib significantly improved survival compared to controls. The generalized Wilcoxon test compared the survival of mice treated with and without dasatinib (P = .0139).*

i Comparison	Difference Between Means	Simultaneous 95% Confidence Limits		
K27M - HGG	0.32	-0.4233	1.0633	
K27M - PA	0.6163	-0.0373	1.2698	
K27M - MB Group4	0.8413	0.1864	1.4962	***
K27M - MB SHH	1.1197	0.3914	1.848	***
K27M - ETMR	1.3123	0.137	2.4876	***
K27M - MB Group3	1.3373	0.646	2.0286	***
K27M - ATRT	1.5182	0.6599	2.3765	***
K27M - MB WNT	1.7698	0.9295	2.61	***
K27M - Rhabdomyosarcoma	2.4748	1.2995	3.6501	***
K27M - Ewing	2.7773	1.6916	3.863	***
Comparisons significant at the 0.05 level are indicated by ***.				

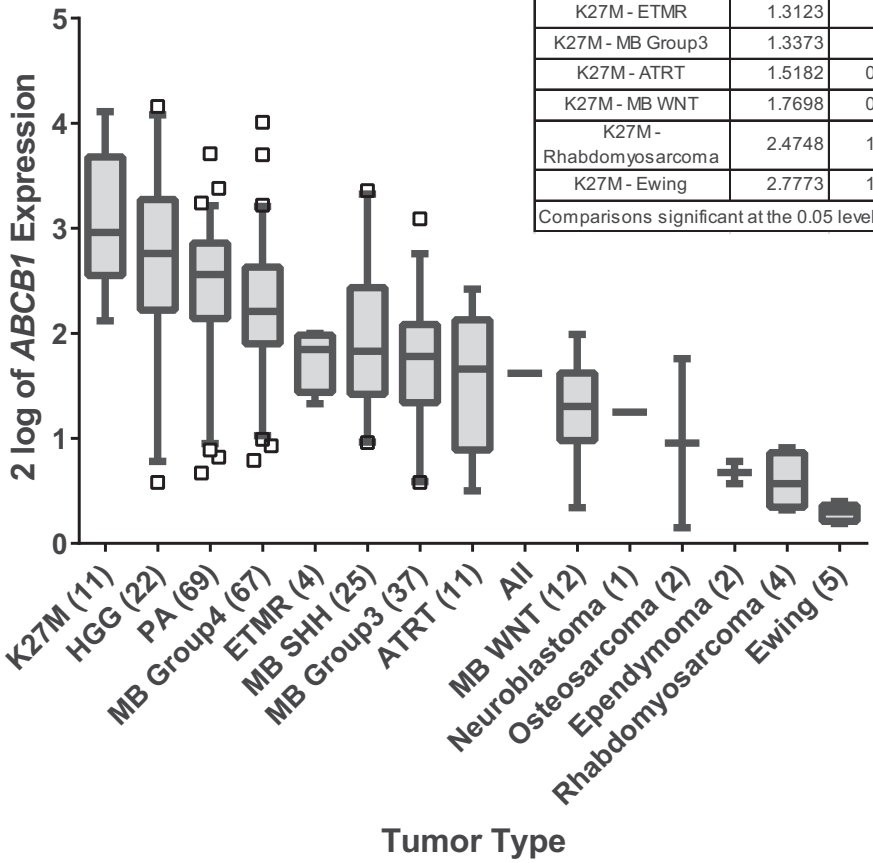

FIGURE 2. *ABCB1 (p-glycoprotein) expression is highest in K27M high-grade gliomas (HGG) in a cohort of 274 pediatric tumors. The mean expression level for each of the 11 pediatric tumor types is displayed with 95% confidence interval. The overall F-test comparing expression levels was statistically significant (P < .0001). Tukey confidence intervals for all pairwise comparisons with K27M are provided. Confidence intervals for all other non-K27M tumor comparisons can be found in* ***Table, Supplemental Digital Content 2****. Patient numbers in parentheses. ATRT = atypical teratoid rhaboid tumor; ETMR = embryonal tumors with multilayered rosettes; MB = medulloblastoma; PA = pilocytics astrocytoma.*

RESULTS

CED Dasatinib Extends Survival

First, we determined that dasatinib had efficacy in H3.3K27M mutant DIPG. Animals with CED catheters attached to continuous delivery pumps infusing dasatinib (n = 8) lived significantly longer than animals with continuous CED delivery of vehicle (n = 6; $P = .0139$; Figure 1) with median OS of 39.5 and 28.5 d, respectively. Histologically, the treatment group had greater cellular proliferation as determined by Ki67 compared to the vehicle group (**Figure**, **Supplemental Digital Content 1**). However, there was no difference in cellular apoptosis as determined by CC3 amongst the groups ($P > .05$; **Figure**, **Supplemental Digital Content 1**).

ABC Transporter Expression in Human DIPG

Using a dataset of 274 pediatric brain and systemic solid tumors,[26] ABCB1, the gene encoding p-glycoprotein, was found

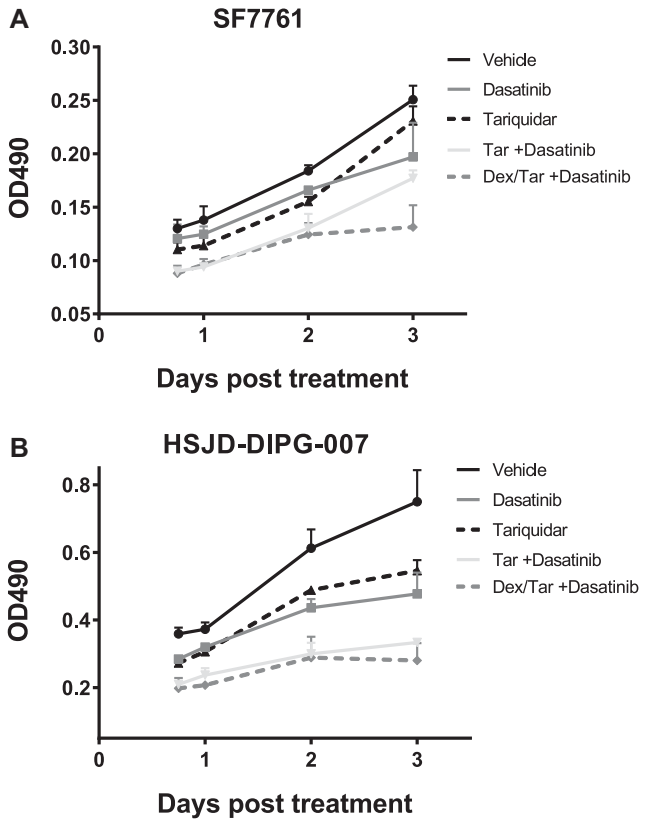

C

Treatment Groups	SF7761 P-value	HSJD-DIPG-007 P-value
Vehicle vs. Dasatinib	< 0.05	< 0.01
Vehicle vs. Tariquidar	ns	< 0.01
Vehicle vs. Tar +Dasatinib	< 0.01	< 0.0001
Vehicle vs. Dex/Tar +Dasatinib	< 0.001	< 0.0001
Dasatinib vs. Tariquidar	ns	ns
Dasatinib vs. Tar +Dasatinib	ns	ns
Dasatinib vs. Dex/Tar +Dasatinib	< 0.05	< 0.05
Tariquidar vs. Tar +Dasatinib	< 0.05	< 0.05
Tariquidar vs. Dex/Tar +Dasatinib	< 0.001	< 0.01
Tar +Dasatinib vs. Dex/Tar +Dasatinib	ns	ns

FIGURE 3. *In Vitro activity of dasatinib, dexamethasone, and tariquidar in 2 H3.327 M mutant DIPG cell lines, SF7761 and HSJD-DIPG-007. MTS assays* **A** *and* **B** *show cellular viability decrease with dasatinib. The effect of dasatinib is further enhanced by adding tariquidar (tar) and dexamethasone (dex). Values shown are the average (mean ± SD) from triplicate samples for each incubation condition.* **C**, *For each separate assay, an ANOVA with Tukey multiple comparison test compared mean levels of cell viability at day 3.*

to have the highest mean expression in K27M mutant high-grade gliomas (HGG), followed closely by wild-type HGG and pilocytic astrocytoma (Figure 2; **Table**; **Supplemental Digital Content 2**). This expression was significantly higher ($P < .05$) than all nongliomas. In comparing wild-type to K27M mutant DIPG samples across 2 independent DIPG datasets of 23 and 21 patients,[27,28] no clear associations across all ABC transporter expression were found (**Figure**, **Supplemental Digital Content 3**).

Dasatinib Plus Dexamethasone and Tariquidar Decrease Cellular Survival In Vitro

Next, we sought to determine the putative effects of adding the p-glycoprotein inhibitor, tariquidar, and dexamethasone to dasatinib in Vitro. Two H3.3K27M mutant DIPG cell lines (SF7761 and HSJD-DIPG-007) were grown over 3 d in vehicle, dasatinib, tariquidar, tariquidar plus dasatinib, and dexamethasone plus tariquidar plus dasatinib. In both cell lines, dasatinib significantly decreased viability in all cell lines compared to vehicle ($P < .05$; Figure 3). The addition of tariquidar and dexamethasone to dasatinib further decreased cell viability compared to vehicle and dasatinib alone ($P < .001$, and $P < .05$, respectively; Figure 3).

Pretreatment With Dexamethasone and Tariquidar Extends Survival

We next validated our in Vitro findings in Vivo. Given our in Vitro results of progressively greater therapeutic efficacy of adding dexamethasone and tariquidar to dasatinib, we selected 3 treatment groups to undergo serial MRI following CED to assess rate of infusate distribution to compare in Vivo: (1) control, (2) CED dasatinib alone, and (3) pretreatment with tariquidar and dexamethasone plus CED dasatinib. This was completed to determine if tariquidar and dexamethasone affected CED infusate clearance. Given the incompatibility of continuous CED pumps with MRI, this was completed as a single-dose CED study. MRI following CED infusion typically yielded a T1-weighted hypointense contrast bolus surrounding the infusion site encompassed by a halo of T1-weighted hyperintense enhancement where contrast was less concentrated (Figure 4A and 4B). We did not identify any differences in infusate dispersion in the pretreatment vs nonpretreatment groups (Figure 4C and 4D).

Following euthanasia, brains were harvested and analyzed histologically. Animals pretreated with tariquidar and dexamethasone had the highest number of CC3 positive, apoptotic cells, per high-power field (mean ± SD) 1050 ± 410, followed by dasatinib alone (785 ± 160), then controls (334.2 ± 109, Figure 5). There was no difference in Ki67 amongst the groups ($P > .05$). Increasing amount of tumor cell apoptosis (CC3) corresponded to increased survival. In comparison to control animals (n = 6), animals treated with dasatinib delivered by single-dose CED infusion (n = 7) had longer survival with median OS of 31.5 and 39 d, respectively. Pretreatment with IP dexamethasone and tariquidar prior to single-dose CED infusion of dasatinib (n = 9) further enhanced survival, extending median OS to 49 d ($P = .0092$, Figure 6). OS results from both

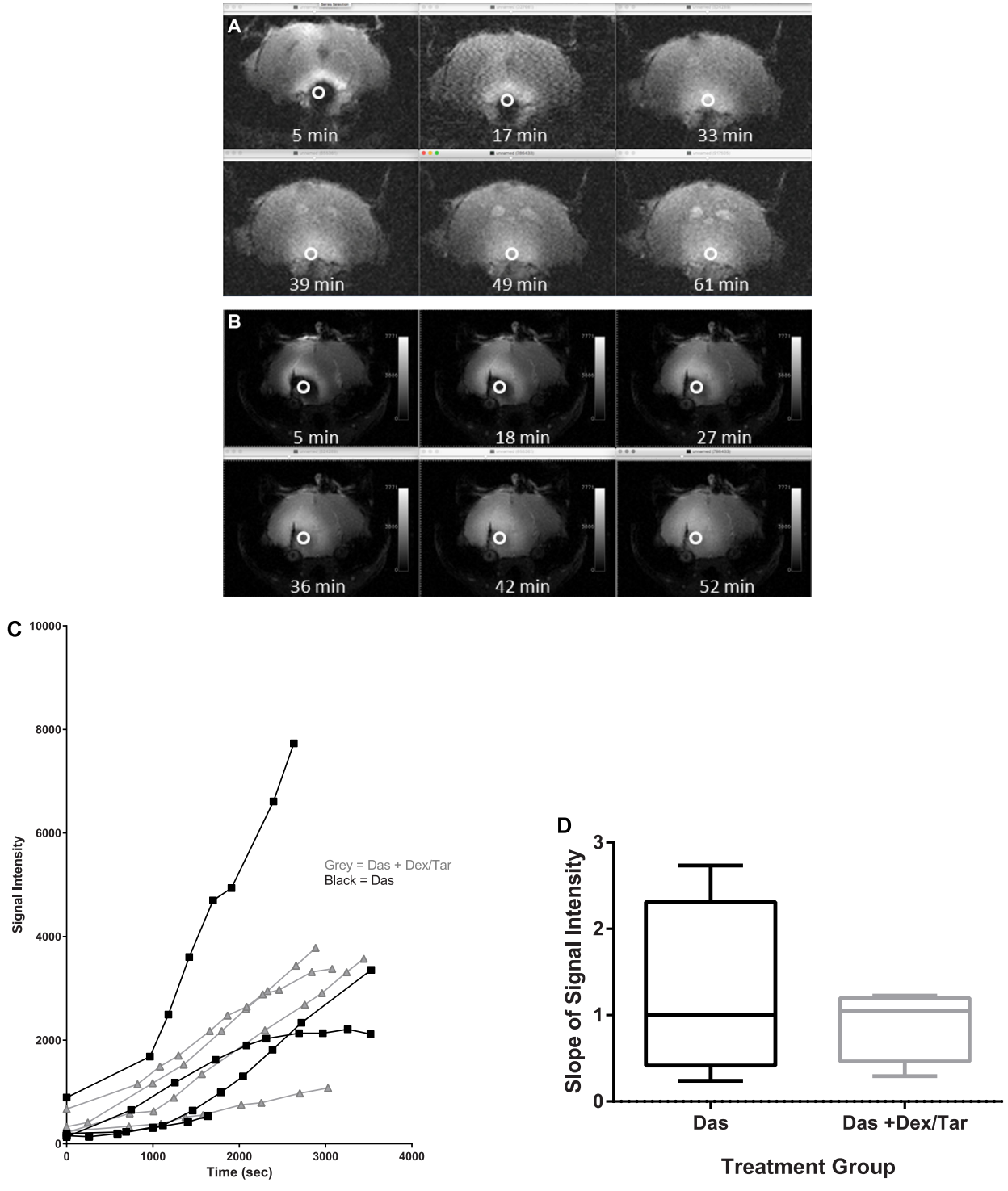

FIGURE 4. *Pretreatment with dexamethasone/tariquidar does not significantly affect CED infusate distribution. Representative serial MRI at multiple time points of* **A**, *an animal that had CED of dasatinib/gadoteridol and* **B**, *an animal pretreated with dexamethasone and tariquidar prior to CED of dasatinib/gadoteridol.* **C**, *There were no differences in the MRI signal intensity curves of animals pretreated with dexamethasone and tariquidar (dex/tar, gray lines) and those not pretreated (black lines).* **D**, *A random coefficient model with an unstructured covariance structure showed no difference in the mean slope of signal intensity within each treatment group, indicating comparable infusate dispersion rates. White circle = region of interest of MRI signal intensity.*

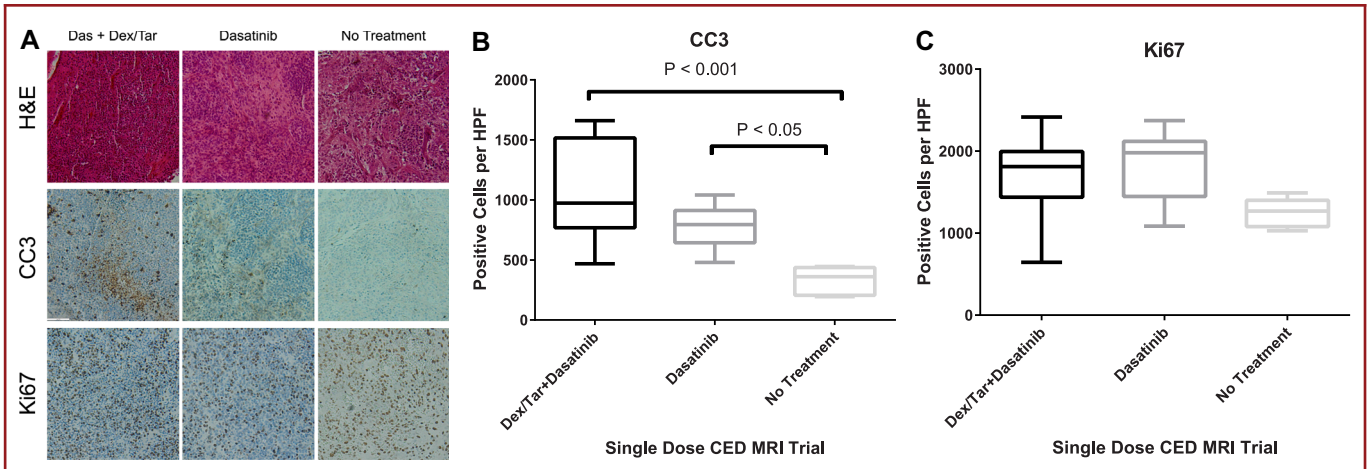

FIGURE 5. **A**, *Representative photos taken at ×10 of murine DIPG stained for hematoxylin/eosin, cleaved caspase 3 (CC3), and Ki67. The greatest amount of intratumoral apoptosis (CC3) was found in the dexamethasone/tariquidar (dex/tar) plus dasatinib group, followed by the dasatinib group, compared to controls. There was no difference in Ki67 amongst groups. Quantification of number of positive-staining CC3* **B** *and Ki67* **C** *cells per high-power field. ANOVA with Tukey post hoc pairwise comparisons was conducted. White bar = 100 μm.*

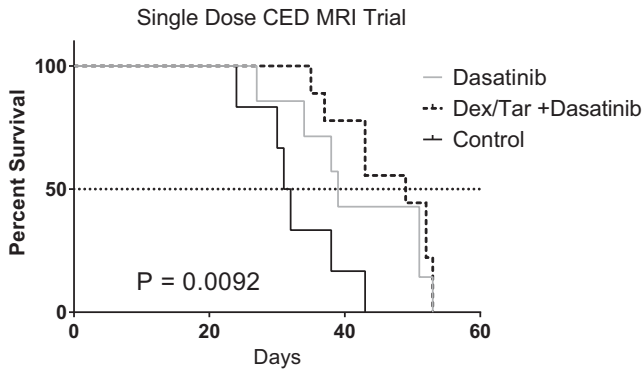

FIGURE 6. *Kaplan–Meier curve of tumor-bearing mice treated with the following: (1) single-dose CED dasatinib; (2) pretreatment of dexamethasone (dex) and tariquidar (tar), followed by single-dose CED dasatinib; or (3) controls. The survival benefit of dasatinib was further enhanced with the pretreatment administration of dexamethasone and tariquidar. The generalized Wilcoxon test survival was observed in each group (P = .0092).*

continuous delivery and single-dose CED studies can be found in Table 1.

DISCUSSION

Despite aggressive investigation, systemic therapies have, to date, failed to meaningfully advance survival for DIPG. As we and other groups have observed, this may be due to failure of adequate drug penetration into the tumor. Although it is possible that DIPG cells are simply resistant to chemotherapy, the efficacy of in Vitro preclinical models[2] contrasted to the poor outcomes seen in clinical trials suggests the possibility of inadequate drug delivery to the tumor. Our group previously showed that BMS754807, a potent multikinase inhibitor, had excellent efficacy against DIPG in Vitro, but the drug did not reach therapeutic levels in Vivo.[30] In clinical studies of dasatinib and VEGFR-2 inhibitor, vandetanib, against DIPG, the CSF: plasma ratio of drug at maximum tolerated doses was approximately 2%;[25] in contrast, the CSF: plasma ratio of temozolomide approaches 20% in adult malignant gliomas.[36]

The lack of a definitive systemic therapy for DIPG has generated considerable interest in CED. The safety of infusing drug into the brainstem has been shown in a variety of animal models[37-43] and in small numbers of children.[13-16] However, in addition to the observation that the BBB of brainstem gliomas is less permeable than genetically identical gliomas in other CNS sites,[44] there is the problem of rapid drug efflux by ABC transporters in DIPG.[6] ABC transporters may also be implicated in drug resistance in nonbrainstem gliomas.[45] We found ABCB1 expression in K27M mutant tumors was not significantly different than other HGGs and pilocytic astrocytomas. These results are in accord with a previous study in which ABCB1 expression was higher in low and high-grade gliomas than medulloblastoma and ependymoma.[46] Implications for this finding include the putative use of p-glycoprotein inhibition as a chemotherapy adjunct for not only DIPG, but also other gliomas.

In this work, we first established that dasatinib is effective via CED in prolonging survival in a murine H3.3K27M mutant DIPG model. We then demonstrated robust ABCB1 (p-glycoprotein) expression in K27M mutant tumors in a large patient cohort. We next demonstrated that the combination of dexamethasone plus ABC transporter inhibition plus tyrosine

TABLE 1. Overall Survival by Treatment Group

Treatment	Single dose CED dasatinib + dex/tar	Continuous CED dasatinib	Single-dose CED dasatinib	Control (no treatment)	Continuous CED vehicle
Number of animals	9	8	7	6	6
Median survival (days)	49	39.5	39	31.5	28.5

kinase inhibition significantly decreased cell viability in Vitro, and resulted in increased tumor cell apoptosis and survival in Vivo. Notably, our group has previously shown that neither dexamethasone[47] nor ABC transporter inhibition[48] alone prolongs survival in rodent models of malignant gliomas. Because we observed no difference in the OS of single CED dasatinib group (median OS 39 d) and the continuous CED dasatinib group (median OS 39.5 d), a direct comparison between dexamethasone/tariquidar pretreatment with continuous CED dasatinib vs continuous CED dasatinib alone was not performed.

Interestingly, in both the continuous CED study (**Figure**, **Supplemental Digital Content 1**) and the single-dose CED study (Figure 5) we found that cellular proliferation as determined by Ki67 was lowest in the control groups. The exact explanation behind this is unclear, but it is possible that Ki67 was higher in the treatment groups because these groups had significantly increased time for tumor growth as indicated by prolonged OS. Indeed, there are numerous reports of the lack of linear correlation between Ki67 and World Health Organization Grade or survival in malignant gliomas.[49-51] Thus, the mechanism of this treatment combination appears to arise not from reduced cellular proliferation but rather from increased cellular apoptosis.

Given the expression of ABC transporters at the BBB in DIPG,[2,6] it is also possible that inhibiting ABC transporters at the BBB resulted in higher concentrations of dasatinib at the tumor. Given the MRI results in this study which demonstrated no appreciable difference in infusate distribution amongst the treatment groups, a less likely explanation would be the putative effect of tariquidar and dexamethasone on slowing CED infusate clearance to increase drug/tumor cell contact time. However, it should be noted that the effects of systemic administration of dexamethasone and tariquidar on CED infusate may have occurred following the 1-h time window in which MRIs were obtained. Regardless, the underpinnings behind the lack of difference in CED infusate distribution between treatment groups are unclear. Future studies will be conducted to further elucidate targeting CED clearance mechanisms to prolong infusate/tumor cell time at delayed time points.

CONCLUSION

Survival of H3.3K27M mutant DIPG-bearing mice treated with CED of dasatinib is improved by inhibiting the ABC transporter p-glycoprotein. These data identify p-glycoprotein as a novel and easily translatable target to improve the efficacy of small molecules delivered via CED for DIPG.

Disclosures

This work was supported by the Southeastern Brain Tumor Foundation (EMT), NIH NS093079 (RH), John McNicholas Pediatric Brain Tumor Foundation (RH), and Rory Deutsch Foundation (OJB). The authors have no personal, financial, or institutional interest in any of the drugs, materials, or devices described in this article.

REFERENCES

1. Johung TB, Monje M. Diffuse intrinsic pontine Glioma: new pathophysiological insights and emerging therapeutic targets. *Curr Neuropharmacol*. 2017;15(1):88-97.
2. Veringa SJ, Biesmans D, van Vuurden DG, et al. In vitro drug response and efflux transporters associated with drug resistance in pediatric high grade glioma and diffuse intrinsic pontine glioma. *PLoS One*. 2013;8(4):e61512.
3. Hargrave D, Bartels U, Bouffet E. Diffuse brainstem glioma in children: critical review of clinical trials. *Lancet Oncol*. 2006;7(3):241-248.
4. Bradley KA, Pollack IF, Reid JM, et al. Motexafin gadolinium and involved field radiation therapy for intrinsic pontine glioma of childhood: A Children's Oncology Group phase I study. *Neuro-oncol*. 2008;10(5):752-758.
5. Harward S, Harrison Farber S, Malinzak M, Becher O, Thompson EM. T2-weighted images are superior to other MR image types for the determination of diffuse intrinsic pontine glioma intratumoral heterogeneity. *Childs Nerv Syst*. 2018;34(3):449-455.
6. Mittapalli RK, Chung AH, Parrish KE, et al. ABCG2 and ABCB1 limit the efficacy of dasatinib in a PDGF-B-driven brainstem glioma model. *Mol Cancer Ther*. 2016;15(5):819-829.
7. Information NCfB. Tariquidar. *PubChem Compound Database*; *CID = 148201* 2018; https://pubchem.ncbi.nlm.nih.gov/compound/148201#section=Top. Accessed June 26, 2018.
8. Fox E, Widemann BC, Pastakia D, et al. Pharmacokinetic and pharmacodynamic study of tariquidar (XR9576), a P-glycoprotein inhibitor, in combination with doxorubicin, vinorelbine, or docetaxel in children and adolescents with refractory solid tumors. *Cancer Chemother Pharmacol*. 2015;76(6):1273-1283.
9. Muz B, Kusdono HD, Azab F, et al. Tariquidar sensitizes multiple myeloma cells to proteasome inhibitors via reduction of hypoxia-induced P-gp-mediated drug resistance. *Leukemia Lymphoma*. 2017;58(12):2916-2925.
10. Zhang Y, Sriraman SK, Kenny HA, Luther E, Torchilin V, Lengyel E. Reversal of chemoresistance in ovarian cancer by co-delivery of a P-glycoprotein inhibitor and paclitaxel in a liposomal platform. *Mol Cancer Ther*. 2016;15(10):2282-2293.
11. Kelly RJ, Draper D, Chen CC, et al. A pharmacodynamic study of docetaxel in combination with the P-glycoprotein antagonist tariquidar (XR9576) in patients with lung, ovarian, and cervical cancer. *Clin Cancer Res*. 2011;17(3):569-580.
12. Walker J, Martin C, Callaghan R. Inhibition of P-glycoprotein function by XR9576 in a solid tumour model can restore anticancer drug efficacy. *Eur J Cancer*. 2004;40(4):594-605.
13. Anderson RC, Kennedy B, Yanes CL, et al. Convection-enhanced delivery of topotecan into diffuse intrinsic brainstem tumors in children. *J Neurosurg Pediatr*. 2013;11(3):289-295.
14. Barua NU, Lowis SP, Woolley M, O'Sullivan S, Harrison R, Gill SS. Robot-guided convection-enhanced delivery of carboplatin for advanced brainstem glioma. *Acta Neurochir*. 2013;155(8):1459-1465.

15. Chittiboina P, Heiss JD, Warren KE, Lonser RR. Magnetic resonance imaging properties of convective delivery in diffuse intrinsic pontine gliomas. *J Neurosurg Pediatr*. 2014;13(3):276-282.
16. Lonser RR, Warren KE, Butman JA, et al. Real-time image-guided direct convective perfusion of intrinsic brainstem lesions. *J Neurosurg*. 2007;107(1):190-197.
17. Paugh BS, Broniscer A, Qu C, et al. Genome-wide analyses identify recurrent amplifications of receptor tyrosine kinases and cell-cycle regulatory genes in diffuse intrinsic pontine glioma. *J Clin Oncol*. 2011;29(30):3999-4006.
18. Puget S, Philippe C, Bax DA, et al. Mesenchymal transition and PDGFRA amplification/mutation are key distinct oncogenic events in pediatric diffuse intrinsic pontine gliomas. *PLoS One*. 2012;7(2):e30313.
19. Zarghooni M, Bartels U, Lee E, et al. Whole-genome profiling of pediatric diffuse intrinsic pontine gliomas highlights platelet-derived growth factor receptor alpha and poly (ADP-ribose) polymerase as potential therapeutic targets. *J Clin Oncol*. 2010;28(8):1337-1344.
20. Becher OJ, Hambardzumyan D, Walker TR, et al. Preclinical evaluation of radiation and perifosine in a genetically and histologically accurate model of brainstem glioma. *Cancer Res*. 2010;70(6):2548-2557.
21. Becher OJ, Hambardzumyan D, Fomchenko EI, et al. Gli activity correlates with tumor grade in platelet-derived growth factor-induced gliomas. *Cancer Res*. 2008;68(7):2241-2249.
22. Zhou Z, Ho SL, Singh R, Pisapia DJ, Souweidane MM. Toxicity evaluation of convection-enhanced delivery of small-molecule kinase inhibitors in naïve mouse brainstem. *Childs Nerv Syst*. 2015;31(4):557-562.
23. Koschmann C, Zamler D, MacKay A, et al. Characterizing and targeting PDGFRA alterations in pediatric high-grade glioma. *Oncotarget*. 2016;7(40):65696-65706.
24. Truffaux N, Philippe C, Paulsson J, et al. Preclinical evaluation of dasatinib alone and in combination with cabozantinib for the treatment of diffuse intrinsic pontine glioma. *Neuro Oncol*. 2015;17(7):953-964.
25. Broniscer A, Baker SD, Wetmore C, et al. Phase I trial, pharmacokinetics, and pharmacodynamics of vandetanib and dasatinib in children with newly diagnosed diffuse intrinsic pontine glioma. *Clin Cancer Res*. 2013;19(11):3050-3058.
26. Grobner SN, Worst BC, Weischenfeldt J, et al. The landscape of genomic alterations across childhood cancers. *Nature*. 2018;555(7696):321-327.
27. Buczkowicz P, Hoeman C, Rakopoulos P, et al. Genomic analysis of diffuse intrinsic pontine gliomas identifies three molecular subgroups and recurrent activating ACVR1 mutations. *Nat Genet*. 2014;46(5):451-456.
28. Zhang L, Chen LH, Wan H, et al. Exome sequencing identifies somatic gain-of-function PPM1D mutations in brainstem gliomas. *Nat Genet*. 2014;46(7):726-730.
29. Veldhuijzen van Zanten SE, Cruz O, Kaspers GJ, Hargrave DR, van Vuurden DG, Network SD. State of affairs in use of steroids in diffuse intrinsic pontine glioma: an international survey and a review of the literature. *J Neurooncol*. 2016;128(3):387-394.
30. Halvorson KG, Barton KL, Schroeder K, et al. A high-throughput in vitro drug screen in a genetically engineered mouse model of diffuse intrinsic pontine glioma identifies BMS-754807 as a promising therapeutic agent. *PLoS One*. 2015;10(3):e0118926.
31. Barton KL, Misuraca K, Cordero F, et al. PD-0332991, a CDK4/6 inhibitor, significantly prolongs survival in a genetically engineered mouse model of brainstem glioma. *PLoS One*. 2013;8(10):e77639.
32. Misuraca KL, Cordero FJ, Becher OJ. Pre-Clinical models of diffuse intrinsic pontine glioma. *Front Oncol*. 2015;5:172.
33. Lewis PW, Muller MM, Koletsky MS, et al. Inhibition of PRC2 activity by a gain-of-function H3 mutation found in pediatric glioblastoma. *Science*. 2013;340(6134):857-861.
34. Asthagiri AR, Walbridge S, Heiss JD, Lonser RR. Effect of concentration on the accuracy of convective imaging distribution of a gadolinium-based surrogate tracer. *J Neurosurg*. 2011;115(3):467-473.
35. Crowley LC, Waterhouse NJ. Detecting cleaved caspase-3 in apoptotic cells by flow cytometry. *Cold Spring Harb Protoc*. 2016;2016(11): pdb.prot087312.
36. Ostermann S, Csajka C, Buclin T, et al. Plasma and cerebrospinal fluid population pharmacokinetics of temozolomide in malignant glioma patients. *Clin Cancer Res*. 2004;10(11):3728-3736.
37. Zhou Z, Singh R, Souweidane MM. Convection-enhanced delivery for diffuse intrinsic pontine glioma treatment. *Curr Neuropharmacol*. 2017;15(1):116-128.
38. Sandberg DI, Edgar MA, Souweidane MM. Convection-enhanced delivery into the rat brainstem. *J Neurosurg*. 2002;96(5):885-891.
39. Souweidane MM, Occhiogrosso G, Mark EB, Edgar MA. Interstitial infusion of IL13-PE38QQR in the rat brain stem. *J Neurooncol*. 2004;67(3):287-293.
40. Souweidane MM, Occhiogrosso G, Mark EB, Edgar MA, Dunkel IJ. Interstitial infusion of carmustine in the rat brain stem with systemic administration of O-benzylguanine. *J Neurooncol*. 2004;67(3):319-326.
41. Luther N, Cheung NK, Dunkel IJ, et al. Intraparenchymal and intratumoral interstitial infusion of anti-glioma monoclonal antibody 8H9. *Neurosurgery*. 2008;63(6):1166-1174; discussion 1174.
42. Luther N, Cheung NK, Souliopoulos EP, et al. Interstitial infusion of glioma-targeted recombinant immunotoxin 8H9scFv-PE38. *Mol Cancer Ther*. 2010;9(4):1039-1046.
43. Ho SL, Singh R, Zhou Z, Lavi E, Souweidane MM. Toxicity evaluation of prolonged convection-enhanced delivery of small-molecule kinase inhibitors in naïve rat brainstem. *Childs Nerv Syst*. 2015;31(2):221-226.
44. Subashi E, Cordero FJ, Halvorson KG, et al. Tumor location, but not H3.3K27M, significantly influences the blood-brain-barrier permeability in a genetic mouse model of pediatric high-grade glioma. *J Neurooncol*. 2015;126(2):243-251.
45. Decleves X, Amiel A, Delattre JY, Scherrmann JM. Role of ABC transporters in the chemoresistance of human gliomas. *Curr Cancer Drug Targets*. 2006;6(5):433-445.
46. Griesinger AM, Birks DK, Donson AM, et al. Characterization of distinct immunophenotypes across pediatric brain tumor types. *J Immunol*. 2013;191(9):4880-4888.
47. Thompson EM, Pishko GL, Muldoon LL, Neuwelt EA. Inhibition of SUR1 decreases the vascular permeability of cerebral metastases. *Neoplasia*. 2013;15(5):535-543.
48. Mittapalli RK, Chung AH, Parrish KE, et al. ABCG2 and ABCB1 limit the efficacy of dasatinib in a PDGF-B-Driven brainstem glioma model. *Mol Cancer Ther*. 2016;15(5):819-829.
49. Mastronardi L, Guiducci A, Puzzilli F, Ruggeri A. Relationship between Ki-67 labeling index and survival in high-grade glioma patients treated after surgery with tamoxifen. *J Neurosurg Sci*. 1999;43(4):819-829.
50. Stoyanov GS, Dzhenkov DL, Kitanova M, Donev IS, Ghenev P. Correlation between Ki-67 Index, world health organization grade and patient survival in glial tumors with astrocytic differentiation. *Cureus*. 2017;9(6):e1396.
51. Tsidulko AY, Kazanskaya GM, Kostromskaya DV, et al. Prognostic relevance of NG2/CSPG4, CD44 and Ki-67 in patients with glioblastoma. *Tumour Biol*. 2017;39(9):1010428317724282.

Acknowledgments

The authors wish to thank Jing Zhang, Khalima Sadieva, and Guo Hu for technical assistance.

Supplemental digital content *is available for this article at www.neurosurgeryonline.com.*

Supplemental Digital Content 1. **Figure**. Comparison of the CED continuous pump groups. ANOVA was conducted. Top panel: Ki67 was higher in the treatment group compared to the vehicle group. Bottom panel: There was no difference in cleaved caspase 3 (CC3) expression between treatment and control. Das = dasatinib; Veh = vehicle.

Supplemental Digital Content 2. Table. Tukey confidence intervals for all pairwise comparisons not involving K27M. See Figure 2.

Supplemental Digital Content 3. **Figure**. Heatmaps of mRNA ABC transporter expression in 2 independent datasets demonstrate no clear association between mutant (red, y-axis) and wild-type K27M DIPG (white, y-axis). A GSE50021[27] and B GSE50774.[28]

COMMENT

In this interesting paper, the authors provide insight to improve the treatment efficacy with convection-enhanced delivery (CED) in an animal model of diffuse intrinsic pontine glioma. The methodology and its development are thoughtful and well presented. Authors found that the addition of tariquidar (ATP-binding cassette transporter inhibitor) and dexamethasone to the CED dasatinib increases the overall survival in H3.3K27M murine model. Interestingly, it does not increase the diffusion of the drug, as would be expected, so the authors hypothesize that this combination has a synergic effect, enhancing the tumor cellular apoptosis and subsequently leading to an increase in the overall survival. As with any situation in which the results do not follow the initial hypothesis, it opens the horizon for further studies to elucidate the mechanism underlaying this synergic effect beyond the increase in apoptosis. It would also be interesting to confirm that there is not a real effect on the diffusion of dasatinib with intraperitoneal dexamethasone and tariquidar, which continues CED dasatinib, rather than a single dose. The authors thoughtfully justify that there was no impact on the overall survival in prior studies without adjuvant therapy between the groups single dose vs continued CED dasatinib. However, because CED is a time-dependent process, continued CED with adjuvant therapy may be worth considering for future studies. We congratulate the authors for this well-supported research in one of the most challenging diseases we, who treat children with brain tumors, all have to face.

Guillermo Aldave
Houston, Texas